Eur. Phys. J. B (2015) 88: 231
DOI: 10.1140/epjb/e2015-60356-2

THE EUROPEAN PHYSICAL JOURNAL B

Regular Article

Floquet analysis of pulsed Dirac systems: a way to simulate rippled graphene

Tridev Mishra, Tapomoy Guha Sarkar, and Jayendra N. Bandyopadhyay[a]

Department of Physics, Birla Institute of Technology and Science, 333031 Pilani, India

Received 5 May 2015 / Received in final form 18 July 2015
Published online 16 September 2015 – © EDP Sciences, Società Italiana di Fisica, Springer-Verlag 2015

Abstract. The low energy continuum limit of graphene is effectively known to be modeled using the Dirac equation in $(2+1)$ dimensions. We consider the possibility of using a modulated high frequency periodic driving of a two-dimensional system (optical lattice) to simulate properties of rippled graphene. We suggest that the Dirac Hamiltonian in a curved background space can also be effectively simulated by a suitable driving scheme in an optical lattice. The time dependent system yields, in the approximate limit of high frequency pulsing, an effective time independent Hamiltonian that governs the time evolution, except for an initial and a final kick. We use a specific form of 4-phase pulsed forcing with suitably tuned choice of modulating operators to mimic the effects of curvature. The extent of curvature is found to be directly related to ω^{-1} the time period of the driving field at the leading order. We apply the method to engineer the effects of curved background space. We find that the imprint of curvilinear geometry modifies the electronic properties, such as LDOS, significantly. We suggest that this method shall be useful in studying the response of various properties of such systems to non-trivial geometry without requiring any actual physical deformations.

1 Introduction

Quantum systems subjected to high-frequency periodic driving have become a prominent feature of quantum simulation studies [1,2]. These studies are mostly aimed at modelling various unique condensed-matter systems [3,4]. Floquet theory and its applications have been extensively studied [5]. Field induced driving [6], or that generated through mechanical straining, for instance, in graphene [7–11] have demonstrated their ability to create novel gauge structures and modify the energy spectra. Such driving schemes have hence become increasingly popular in cold atom and ion-trap systems as a means of implementing effective potentials that could simulate magnetic fields or spin-orbit couplings [12–19]. The theoretical formalism underlying these driven quantum systems relies on a time dependent forcing that synthesizes an effective approximate time independent Hamiltonian [20–27]. A recent trend in these investigations has been inclined towards looking at a variety of driving schemes to explore potentially interesting Hamiltonians [28].

In much of the last decade two areas have witnessed rapid progress, namely, the physics of graphene with its applications [29] and ultra cold atoms in optical lattices [30]. Interest in the former is driven by the realization of a perfectly flat two-dimensional (2D) system and the unique physics observed in the material due to its relativistic dispersion relation [31–33]. Optical lattices, on the other hand, has offered an indispensable simulator for realizing many-body condensed matter phenomena and noting their response to a highly controllable variation of system parameters. This has motivated a significant advancement in the efforts to simulate graphene like systems in optical lattice [34–43]. Graphene systems have been studied in the presence of time dependent potentials [44,45]. Further graphene is noted to show exotic properties, either under mechanical strain, curvature or possessing defects such as dislocations [7–11,46–55]. These studies often use a continuum model of Dirac fermions in curved $(2+1)$ dimensions in the limit of low energy excitations. This has also been investigated in the cold atom/optical lattice setup with the objective of studying relativistic electrodynamics in the presence of gravity [56].

The experimental realization of such systems has presented technical difficulties arising from the spin-like and position dependent nature of the nearest-neighbor hopping amplitude in their Fermi-Hubbard Hamiltonian. The essential requirement is the coupling of an artificial non-abelian gauge field to the ultra cold fermionic atoms in the optical lattice (near half-filling) giving rise to the appropriate effective dynamics [57–65].

A key ingredient of all such simulations involves the generation of artificial gauge fields in optical lattices through periodic driving or "shaking" [17,66–68]. We propose the use of a certain driving scheme to obtain an effective curved graphene model in the optical lattice

[a] e-mail: jnbandyo@gmail.com

setup. The key distinction of our proposed scheme from similar works [56] is our use of pulse sequences with suitably chosen modulating operators, as described in reference [28], to generate the effects of smooth driving. This is suggested as an alternate scheme to circumvent difficulties arising from the complicated form of the effective tunneling parameter in conventional treatments. An added advantage of this method is the easy correspondence afforded by it between the continuum and the lattice using a suitable map relating the operators in the two pictures.

In this work, we outline a scheme for the generation of an approximate effective Hamiltonian using periodic time dependent forcing on a fermionic 2D optical lattice having the Bloch band topology of flat graphene such that the resulting static effective system mimics the features of a curved background. To compare with the Dirac equation in curved $(2+1)$ dimensional background we consider a metric with a conformally flat spatial part. The Dirac equation in this curved background is cast in a Hamiltonian form to allow easy comparison with the lattice Hamiltonian in the continuum limit. The effects of background curvature are noted. We have found an effective approximate time-independent Hamiltonian which is obtained from a specific high frequency time-periodic driving of the flat space Dirac Hamiltonian. This effective Hamiltonian is found to be identical to the Dirac Hamiltonian in curved space at the leading order.

We also note the direct correspondence between the nature and the periodicity of the driving to the form and the extent of curvature. The modification of the electronic properties, specifically Local Density of States (LDOS) is studied in low energy regimes near the Fermi points.

2 Formalism

2.1 Massless Dirac equation in curved $(2+1)$ D space

We consider the effects of curvature of the background space on the massless Dirac equation. The curved space Dirac Hamiltonian is believed to govern the quasi-particle (i.e., the massless Dirac fermion) dynamics in the continuum limit of the low energy approximation for graphene sheets with curvature. In the subsequent sections, we shall elaborate upon our intent to replicate such systems in the framework of optical lattice simulation.

The Dirac equation in $(2+1)$ dimensional space-time has been studied in various contexts and has a well defined formalism [69–77]. This section provides a brief overview of this as relevant to our work. We consider a $(2+1)$ dimensional space-time as the backdrop for our analysis. We choose a space-time metric of the form

$$ds^2 = dt^2 - e^{-2\Lambda(x,y)}\left(dx^2 + dy^2\right), \tag{1}$$

where t represents the time coordinate, x and y are the spatial isothermal Cartesian coordinates, and $e^{-2\Lambda(x,y)}$ denotes the conformal factor. We note here that the two-dimensional spatial part of this metric $\mathrm{diag}\,(1, -e^{-2\Lambda(x,y)}, -e^{-2\Lambda(x,y)})$ is completely general in representing two-dimensional curved surfaces. This metric has been used in the context of studying Dirac equation coupled to curved space-time [78] with a distribution of defects, for instance, in the case of corrugated graphene sheets [7–9].

The Dirac equation in curved space-time takes the form

$$i\gamma^{\mu}(x)\left(\partial_{\mu} + \Gamma_{\mu}(x)\right)\psi = 0. \tag{2}$$

The spin connection term, $\Gamma_{\mu}(x)$, is given by reference [78]

$$\Gamma_{\mu}(x) = g_{\lambda\alpha}\left(e^{i}_{\nu,\mu}E^{\alpha}_{i} - \Gamma^{\alpha}_{\nu\mu}\right)s^{\lambda\nu} + a_{\mu}\mathcal{I} \tag{3}$$

where e^{i}_{ν} and E^{α}_{i} denote the usual vielbeins and their inverses respectively, $\Gamma^{\alpha}_{\nu\mu}$ are the Christoffel connection coefficients and $s^{\lambda\nu}$ are the generators of spinor transformation in curved space-time. This expression illustrates the indeterminacy of the connection term to upto a constant a_{μ}. Hence Γ_{μ} has an arbitrary trace [78]. This offers a gauge freedom which can be exploited depending on the nature of the problem. We take the standard choice for Γ_{μ} as:

$$\Gamma_{\mu}(x) = \frac{1}{2}g_{\lambda\alpha}\left(e^{i}_{\nu,\mu}E^{\alpha}_{i} - \Gamma^{\alpha}_{\nu\mu}\right)s^{\lambda\nu} \tag{4}$$

with,

$$s^{\lambda\nu}(x) = \frac{1}{2}\left[\gamma^{\lambda}(x), \gamma^{\nu}(x)\right]. \tag{5}$$

The γ matrices with curved space-time indices are related to the usual Dirac matrices in flat space by $\gamma^{\mu}(x) = E^{\mu}_{i}(x)\gamma^{i}$. We choose the following representation using the Pauli matrices for the γ^{i}s

$$\gamma^{0} = \sigma^{z} \quad \gamma^{1} = i\sigma^{y} \quad \gamma^{2} = -i\sigma^{x}. \tag{6}$$

In our choice of representation, σ^{z} is diagonal and σ^{y} is complex.

The spin connection components, for our metric (see Eq. (1)), are given as:

$$\Gamma_{1}(x) = \frac{i}{2}\frac{\partial\Lambda(x,y)}{\partial y}\sigma^{z}, \ \Gamma_{2}(x) = -\frac{i}{2}\frac{\partial\Lambda(x,y)}{\partial x}\sigma^{z}. \tag{7}$$

The massless Dirac equation in curved $(2+1)$ space-time, can hence be written as:

$$\left[i\sigma^{z}\frac{\partial}{\partial t} - e^{\Lambda(x,y)}\left(\sigma^{y}\frac{\partial}{\partial x} - \sigma^{x}\frac{\partial}{\partial y}\right) + \frac{e^{\Lambda(x,y)}}{2}\left(\frac{\partial\Lambda(x,y)}{\partial y}\sigma^{x} - \frac{\partial\Lambda(x,y)}{\partial x}\sigma^{y}\right)\right]\psi = 0, \tag{8}$$

where we have used equations (2) and (4). This equation can be recast in an explicitly Hamiltonian form by breaking the manifestly covariant form as:

$$i\frac{\partial\psi}{\partial t} = e^{\Lambda(x,y)}\left[-i\sigma^{j}\partial_{j} - \frac{i}{2}\left(\frac{\partial\Lambda(x,y)}{\partial y}\sigma^{y} + \frac{\partial\Lambda(x,y)}{\partial x}\sigma^{x}\right)\right]\psi. \tag{9}$$

The entire operator acting on ψ in the RHS of the above equation may be interpreted as the Dirac Hamiltonian in curved space. This Hamiltonian is required to be synthesized using the driven optical lattice. As will be shown later it is possible to formulate a driving scheme which does exactly this. In the following section we discuss a procedure for obtaining an effective time-independent Hamiltonian for periodically driven systems. This shall find appropriate implementation in optical lattices.

2.2 Periodic pulsing and effective Hamiltonians

In the study of quantum systems having periodic time dependent Hamiltonians [22,23], a special category is devoted to the class of systems where the system is subjected to high frequency periodic forcing [20]. The theoretical treatment of such systems has its roots in the study of similar classical systems [79,80]. The literature suggests various routes to arrive at an effective time-independent Hamiltonian [21,24–26]. The traditional practice of using the Cambell-Baker-Hausdorff (CBH) expansion or Trotter expansion to study Floquet systems has certain inherent defects [26,27]. A recent approach [28], inspired by reference [26], forms the basis of our formalism. It uses the idea of engineering effective Hamiltonians by applying carefully selected periodic driving schemes to quantum systems, geared towards generating desired effective static systems.

To start with, we consider a time-periodic Hamiltonian $H(t)$ that can be written as:

$$H(t) = H_0 + V(t), \tag{10}$$

where H_0 is time independent and $V(t)$ is the periodic time dependent part such that $V(t+T) = V(t)$. The periodic time-dependent operator $V(t)$ can be expanded in a Fourier series as:

$$V(t) = V_0 + \sum_{1\le n<\infty} \hat{V}_n e^{in\omega t} + \sum_{1\le n<\infty} \hat{V}_{-n} e^{-in\omega t}. \tag{11}$$

In order to obtain the effective time independent Hamiltonian one writes the time evolution operator as:

$$U(t_i, t_f) = e^{-i\hat{F}(t_f)} e^{-i\hat{H}_{eff}(t_f - t_i)} e^{i\hat{F}(t_i)}, \tag{12}$$

where, one introduces a time dependent Hermitian operator $\hat{F}$. The idea is to push all the time dependence to the initial and final "kick" terms and render the main time evolution to be dictated by a time independent Hamiltonian. The systematic formalism (see Appendix) yields the following expression for the effective Hamiltonian [28]

$$H_{eff} = H_0 + V_0 + \frac{1}{\omega}\sum_{n=1}^{\infty}\frac{1}{n}\left[\hat{V}_n, \hat{V}_{-n}\right] + \frac{1}{2\omega^2}\sum_{n=1}^{\infty}\frac{1}{n^2}\left(\left[\left[\hat{V}_n, H_0\right], \hat{V}_{-n}\right] + h.c.\right) + \mathcal{O}(\omega^{-3}). \tag{13}$$

The correction terms that appear in the effective Hamiltonian depend on the commutator of the Fourier coefficients $\hat{V}_n$ with each other and with the unperturbed Hamiltonian H_0. It is worth noting, that, for potentials which have time-reversal symmetry ($V(t) = V(-t)$) equation (11) imposes restrictions on the coefficients so that the commutator $[\hat{V}_n, \hat{V}_{-n}]$ vanishes. For such potentials the leading order correction is $\mathcal{O}(\omega^{-2})$. The appearance of the $\mathcal{O}(\omega^{-1})$ term with a non-zero coefficient is a feature of potentials with dependence on momentum operators in addition to position and time. Time reversal symmetry is broken in these cases. Several possible choices for such potentials are worked out in reference [28]. Our choice of driving potential, discussed in the latter portion of this work, falls into this category. This serves as a helpful reminder of the occasional deviations from the intuitively expected $\mathcal{O}(\omega^{-2})$ leading order correction in the effective Hamiltonian, which is expected for potentials with time reversal symmetry.

We shall now focus on a specific kind of forcing potential. The driving potential $V(t)$ shall be considered to be a sequence of pulses that repeat periodically. The choice of the number of phases in a given pulse sequence dictates the form of the effective Hamiltonian. This offers a wide variety of possibilities up to a given order ω^{-1} in the perturbation expansion.

Let us consider a general N-phase pulse sequence, with period T, of the form

$$V(t) = \sum_{r=1}^{N} f_r(t) V_r \tag{14}$$

where f_r denotes a square profile such that

$$f_r(t) = \begin{cases} 1, & (r-1)T/N \le t \le rT/N, \\ 0, & \text{elsewhere.} \end{cases} \tag{15}$$

Here, V_r are arbitrary operators that are free to be chosen as per ones requirement. Each phase lasts for a duration of T/N. We also impose the condition $\sum_{r=1}^{N} V_r = 0$.

The time-dependent Hamiltonian for such a choice of driving is then

$$H(t) = H_0 + \sum_{r=1}^{N} f_r(t) V_r. \tag{16}$$

Using the Fourier series expansion this can be written as:

$$H(t) = H_0 + \sum_{n\neq 0} \hat{V}_n e^{in\omega t}, \tag{17}$$

where

$$\hat{V}_n = \frac{1}{2\pi i}\sum_{r=1}^{N}\frac{1}{n} e^{-2\pi i n r/N}(e^{2\pi i n/N} - 1) V_r. \tag{18}$$

It is possible to use equation (13) at this stage to obtain a generic expression for the time-independent effective Hamiltonian for the kind of driving given in equation (14) (Eq. (30) in Ref. [28]).

Given the flexibility of choosing the number of phases and also the modulating operators, a wide variety of effective Hamiltonians can be generated. The next section deals with one such choice that enables us to design the required gauge field to simulate the physics of curved graphene in optical lattices. The usefulness of such a pulsing scheme is demonstrated by showing its equivalence to an optical lattice shaken/modulated by a smooth driving.

The modulation scheme used in standard optical lattices does not consist of such pulsing and instead uses smooth driving. The effective Hamiltonian obtained for smoothly modulated optical lattices carries an imprint of the modulation frequency through the renormalized hopping term (which is a function of ω). On Taylor expanding the hopping parameter as a series in ω^{-1}, this effective Hamiltonian matches with the one obtained by a pulsing scheme at the leading orders [28].

2.3 Simulating rippled graphene: optical lattice scheme

As mentioned previously, the use of fermionic optical lattices to simulate Dirac cones and massless Dirac fermions is well established. In such a system the application of a time-dependent sinusoidal modulation can be used to obtain novel gauge effects in an artificial time-averaged manner. The possibility of doing this using the method discussed in the previous section is elaborated here.

Among the wide range of choices that do exist, our problem lends itself rather neatly to a 4-phase pulse sequence with modulation of the Hamiltonian given by:

$$\mathcal{P}_4 : \{H_0 + A, H_0 + B, H_0 - A, H_0 - B\}. \tag{19}$$

This compares to equation (14) for $N = 4$ with $V_1 = -V_3 = A$ and $V_2 = -V_4 = B$, where A and B are suitable operators. As discussed in the last section, this is equivalent to a smooth driving of the form

$$V(t) = A\cos(\omega t) + B\sin(\omega t). \tag{20}$$

This choice of the time-dependent potential yields the following effective Hamiltonian [28]

$$H_{eff} = H_0 + \frac{i}{2\omega}[A, B]\frac{1}{4\omega^2}\left([[A, H_0], A] + [[B, H_0], B]\right) + \mathcal{O}(1/\omega^3). \tag{21}$$

It is significant in our context to note that the expression for H_{eff} has both first order and second order terms in ω with the appropriate commutator brackets. The freedom in the choice of A and B allows us to engineer the desired effective Hamiltonian.

The periodic driving scheme has a small parameter ω^{-1}, the time-period of forcing. It is our contention that it is possible to use the formalism of generating effective approximate Hamiltonians, through a choice of suitable operators A and B as mentioned in equation (19), to reproduce a Dirac Hamiltonian in curved space. This would involve choosing an appropriate pulsing scheme.

We note that the low energy limit of a continuum approximation of graphene, as simulated in the lattice, has the Hamiltonian of the form [29]

$$H_{\mathrm{G}} = -iv_F\sigma^j\partial_j \tag{22}$$

in units of $\hbar$, where v_F is the Fermi velocity and $\partial_j = (\partial_x, \partial_y)$ is the gradient operator in 2-dimensions. We shall subsequently work in units where $v_F = 1$. This motivates us to consider the primary Hamiltonian in our analysis as $-i\sigma^j\partial_j$. The discussion here solely employs the continuum formalism for the operators and the mapping to the second quantized forms for the operators and the Hamiltonians are only introduced later in the section on results and discussion.

Let us consider a driving scheme with $H_0 = -i\sigma^j\partial_j$, the Dirac Hamiltonian in flat space and choose the operators A and B of the form

$$A = \sigma^j\alpha_j \qquad B = \sigma^k\beta_k \tag{23}$$

where, $\alpha_j = [i\partial_y, -i\partial_x, 0]$ and $\beta_k = [0, 0, -f(x, y)]$. With this choice, equation (21) yields an approximate effective Hamiltonian H_{eff} up to order ω^{-1} given by:

$$H_{eff} = \frac{1}{2}\left[-i\left(1 + \frac{f(x,y)}{\omega}\right)\sigma^j\partial_j\right] - \frac{1}{2}\left[i\sigma^j\partial_j\left(1 + \frac{f(x,y)}{\omega}\right)\right]. \tag{24}$$

For large ω this is a good approximation. The term of $\mathcal{O}(\omega^{-2})$ is significantly suppressed and manifests as non-trivial couplings and maybe ignored for our present analysis. With a substitution

$$e^{\Lambda(x,y)} = \left(1 + \frac{f(x,y)}{\omega}\right)$$

we have

$$H_{eff} = \frac{1}{2}[-ie^{\Lambda(x,y)}\sigma^j\partial_j - i\sigma^j\partial_j\ e^{\Lambda(x,y)}] \tag{25}$$

such that the entire expression is in terms of $\Lambda(x, y)$ instead of $f(x, y)$. The Hamiltonian in equation (25) can be further simplified and explicitly written as follows

$$H_{eff} = e^{\Lambda(x,y)}\left[-i\sigma^j\partial_j - \frac{i}{2}\left(\frac{\partial\Lambda(x,y)}{\partial y}\sigma^y + \frac{\partial\Lambda(x,y)}{\partial x}\sigma^x\right)\right]. \tag{26}$$

We seek to map this effective time-independent Hamiltonian that is obtained from the original time-dependent Hamiltonian to the Dirac Hamiltonian in curved space. The function $\Lambda(x, y)$ appearing here is expected to be mapped to the metric in some fashion in the equivalent curved space description.

Comparing equations (26) and (9) we establish the correspondence between the periodically driven effective system and a curved space description. The function $\Lambda(x, y)$ that depends on the periodic driving scheme is now seen to appear in the conformal factor of the metric in the curved

space picture. A quantity of geometrical interest describing 2D curved surface is the Gauss curvature $K(x, y)$ given by:

$$K(x, y) = e^{2\Lambda}\nabla^2(\Lambda). \tag{27}$$

This scalar function has complete information about the curved 2D surface. Since $\Lambda = \ln(1 + \frac{f(x,y)}{\omega})$ depends on the driving scheme f and driving frequency ω, the curvature shall depend on these directly. It is hence possible to reproduce the effects of curvature ($K \neq 0$) by suitably manipulating the driving scheme. This completes the mapping between the two equivalent pictures.

In order to confirm that our model suitably mimics the properties of curved graphene, it is required that some physical quantity associated with it be computed and obtained experimentally. We regard the local density of states (LDOS) to be a suitable candidate. In the following we briefly recapitulate its significance and prescribe a method for determining it theoretically.

The LDOS is a quantity of interest in the study of electronic and transport properties of various condensed matter systems. It offers information regarding the spatial variation in the density of states over a region, arising out of local disturbances, that can be verified experimentally using scanning tunneling microscopy (STM) techniques. It is therefore a physically relevant parameter for our study. Our analysis suggests that the electronic properties for a periodically driven graphene like optical lattice system, describable by a Dirac Hamiltonian, shall be the same as one expects for the same system in a curved background without any periodic forcing. To compute the LDOS [81] one first needs to calculate the Green's function for the system, for the case of non-interacting electrons, as follows.

$$G(z, \mathbf{r}, \mathbf{r}') = \sum_n \frac{\psi_n(\mathbf{r})\psi_n^*(\mathbf{r}')}{(z - E_n)} \tag{28}$$

where, z denotes a complex energy variable, ψ_n are energy eigenstates in coordinate representation, E_n represents the energy eigenspectrum and the sum ranges over the n eigenvalues of energy. The expression for the LDOS is given as:

$$\rho(\epsilon, \mathbf{r}) = -\frac{1}{\pi}\mathrm{Im}\sum_n \frac{|\psi(\mathbf{r})|^2}{(\epsilon + i\delta - E_n)} \tag{29}$$

which may be written as

$$\mathrm{LDOS} = \rho(\epsilon, \mathbf{r}) = -\frac{1}{\pi}\mathrm{Im}\left[G(\epsilon + i\delta, \mathbf{r}, \mathbf{r}')\right]. \tag{30}$$

We shall compute the LDOS numerically using the spectrum of the Hamiltonian in equation (26) and compare it with the flat space case where $\Lambda = 0$.

3 Results and discussion

The study of alterations to the electronic properties of graphene sheets as a result of deformation, curvature, defects or impurities focuses chiefly on the modifications to the LDOS or the appearance of a gap at the Fermi points [10,33,47,48,82–87]. These works discuss the possibility of opening a band gap in graphene at the Dirac point, which is known to be topologically protected by inversion and time reversal symmetries [88–90]. The presence of perturbations that respects these discrete symmetries can only move the Fermi points but not create a gap [91]. A hybridization of the Fermi points with opposite topological charge (winding number) allows a subsequent opening of gap [92].

In our present analysis we attempt to examine the effect on the LDOS for graphene-like optical lattice under a periodic driving. The approach has similar motivations to earlier studies on LDOS in rippled graphene [47,48]. The principal difference being that our system does not involve taking a graphene sheet with any curvature or defects but imparting curved-graphene properties to an optical lattice via pulsing. The choice of the driving scheme function $f(x, y)$ that maps to the conformal factor in the metric is taken as:

$$f(x, y) = x^2 + y^2. \tag{31}$$

This choice of the driving scheme is used to compute the curvature according to equation (27) and yields a constant Gaussian curvature $K(x, y) = \frac{4}{\omega}$. Thus the curvature turns out to be inversely proportional to the driving frequency ω. Hence, with our high frequency driving scheme (high frequency is a necessary condition required for the convergence of the perturbation series in Eq. (A.10)) we are able to model a small positive constant curvature.

The deep significance behind the similarity between the Dirac Hamiltonian in curved space and the effective time independent Hamiltonian needs to be addressed. This can be understood by acknowledging that the effects of both curvature and driving find expression through the unifying formalism of effective gauge fields. In the case of a rippled graphene sheet [47,48,51–54] it has been well established that the effect of curvature manifests in the curved space Dirac equation through an artificial magnetic vector potential giving rise to a pseudo-magnetic field. This is a reinterpretation of the contribution coming from the spin connection and the curved space gamma matrices, which characterize the changes to the ordinary flat space derivatives (giving the correct form of the covariant derivatives in curved space). The modification gets carried over into the lattice picture through a phase factor that modulates the hopping term (Peierls phase). This is the usual way to couple a gauge field to a tight binding Hamiltonian.

It is also a matter of fact that periodic driving can indeed replicate gauge structures [28]. A landmark approach [17] maybe used to simulate complex valued hopping parameters with a tunable value for the Peierls phase in the effective time independent lattice Hamiltonian. Thus a scheme for simulating a vector potential that amounts to a finite pseudo-magnetic flux through a 2D lattice is available. Mathematically, the slow part of the eigen states of the Floquet Hamiltonian $-i\hbar\frac{\partial}{\partial t} + H$ are the object of study in the time independent picture. The use

of a unitary gauge transformation $e^{iF(t)}$ (see Appendix) to map the states of the system to a projective space where the evolution of the system is governed by a time independent H_{eff}, essentially involves a transformation of the time evolution operator in a manner similar to the transformation of the momentum operator (i.e. the operator for translation) in the presence of a minimally coupled gauge field. Equation (A.7) is very similar to a gauge transformation. Thus, from a differential geometric point of view, the periodic driving defines its own connection due to which arises a holonomy in the line bundle over the projective space of rays of the Hilbert space [93]. In this manner a gauge invariant time dependent phase appears as corrections to the quasi-energies of the system over time periods large compared to that of the high frequency periodic driving.

It is possible to write down the operators A and B of the driving in the conventional second quantized notation. To do so we adopt a convention in which the fermionic optical lattice Hamiltonian reads

$$H_0 = J \sum_{\langle k,j \rangle} \Psi^\dagger_{k+1,j} \sigma^x \Psi_{k,j} + \Psi^\dagger_{k,j+1} \sigma^y \Psi_{k,j} - h.c. + H_{\text{on-site}} \tag{32}$$

where, J is the plain hopping parameter, a the lattice spacing, $\Psi^\dagger_{k,j} = (\hat{a}^\dagger_{k,j}, \hat{b}^\dagger_{k,j})$ creates a particle at the site (ka, ja) in some spin state. The operators $\hat{a}_{k,j}$ and $\hat{b}_{k,j}$ stand for the two triangular sub-lattices of the optical lattice. The operators A and B in this convention, for the choice of $f(x, y)$ in equation (31), becomes

$$A = -\frac{i}{2a} \sum_{\langle k,j \rangle} \Psi^\dagger_{k,j+1} \sigma^x \Psi_{k,j} - \Psi^\dagger_{k+1,j} \sigma^y \Psi_{k,j} - h.c.$$
$$B = -\sigma^z \frac{a^2}{2} \sum_{\langle k,j \rangle} k^2 \Psi^\dagger_{k+1,j} \sigma^x \Psi_{k,j} + j^2 \Psi^\dagger_{k,j+1} \sigma^y \Psi_{k,j} + h.c. \tag{33}$$

In the above expressions, we make use of the following map between continuum operators and those on the lattice as [28]

$$-i\sigma^x \partial_x \equiv \frac{i}{2a} \sum_{\langle k,j \rangle} \Psi^\dagger_{k+1,j} \sigma^y \Psi_{k,j} - h.c.$$
$$-i\sigma^y \partial_y \equiv \frac{i}{2a} \sum_{\langle k,j \rangle} \Psi^\dagger_{k,j+1} \sigma^x \Psi_{k,j} - h.c. \tag{34}$$

and

$$x^2 + y^2 \equiv \frac{a^2}{2} \sum_{\langle k,j \rangle} k^2 \Psi^\dagger_{k+1,j} \sigma^x \Psi_{k,j} + j^2 \Psi^\dagger_{k,j+1} \sigma^y \Psi_{k,j} + h.c. \tag{35}$$

The mapping between the continuum operators and their lattice counterparts enables the actual possibility of simulation of the Hamiltonian on the lattice.

The issue of experimentally realizing the system as described above is contingent on successful implementation of the lattice operators A and B, followed by a design of the driving which would ultimately yield the desired effective Hamiltonian in the time independent approximation. This has to be approached in an incremental fashion. The operators A and B are themselves constructed from operators for position and momentum in a 2D, fermionic optical lattice. Experimental realization of these operators uses pulsed directional hoppings i.e. time dependent modulation of tunneling [12] by varying the laser intensity in a certain direction. However, in our case the 2×2 character of the Hamiltonian is also to be accounted for. This requires a periodic drive capable of imparting such features.

A scheme, recently suggested, in an effort to simulate spin-orbit coupling (SOC) through periodically driving a tight-binding lattice of neutral ultra-cold atoms [94] may enable this. This uses a spin-dependent periodic driving force, achieved through a time periodic magnetic field coupled to opposite spin states, to generate complex valued tunneling parameters. There is an additional radio frequency coupling between adjacent spin states. The cumulative effect when viewed from the perspective of a time independent effective Hamiltonian is that of an optical lattice with a spin-dependent renormalization of the hopping term. This technique is accompanied with the added advantage of generating a site dependent phase associated with the terms of the Hamiltonian which are associated with tunneling between adjacent sites (this being an essential feature of our Hamiltonian). It must be noted here that the work [94] deals with a 1D lattice, whereas we require the scheme to be adapted for the 2D case.

The procedure, upto this point, manages to realize the operators A and B in a time averaged manner. In order to further set up our curved space Hamiltonian we have to resort to alternating between the two operators in the manner of the 4-phase pulse sequence discussed in Section 2.3. Thus another layer of time averaging will be required to arrive at our desired Hamiltonian. The pulsing may be devised such that during the phase when A is supposed to act we use a combination of laser tuned tunneling and radio frequency tuning and for B just the SOC modelling technique be used. The need to work with multiple time scales is apparent here and one is required to average through these to get at the desired Hamiltonian over a prolonged duration. The issues related to cooling and the spontaneous emission of photons are claimed to be partially overcome in the SOC modelling technique discussed above as compared to near-resonant Raman laser coupling schemes. However, periodic driving does create excitations in the system which may lead to spontaneous emission. This is influenced by the driving frequency, lattice modulation and interactions between particles (see Refs. in [94]). The experimental viability of sustaining multiple time scales in the system to obtain the desired dynamics over a reasonable duration of time without undue heating and excitations has to be further looked into and is beyond the scope of the present work.

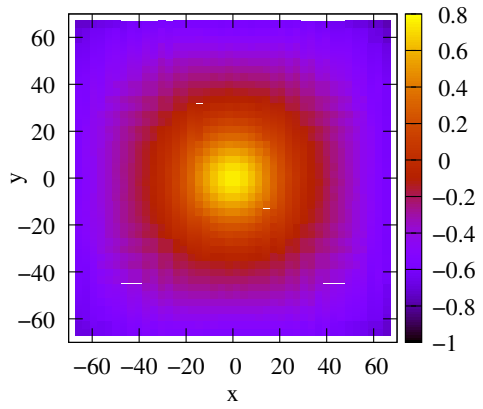

Fig. 1. Correction to the LDOS given by $\frac{\rho}{\rho_o} - 1$ with ρ being the LDOS for pulsed graphene and ρ_o that for ordinary graphene.

It also remains to be seen how the approach suggested above compares with the purely spatial techniques elaborated in reference [56]. One of these is to use the magnetic field induced Zeeman splitting of the hyperfine levels and design the system as a bichromatic spin-independent super-lattice. The fermi gas of atoms used can be made to populate various sublevels and transition between them via laser induced tunneling. The spatially dependent nature of the tunneling is ensured by making the Raman laser detunings hence Zeeman splittings spatially dependent. This method however, besides its inherent technical complexity, has to contend with issues of stability and the lifetime of atomic excitations owing to spontaneous emission of photons. An alternative method, also put forward in the same work, considers using the waist spread of laser beams to generate tunneling terms. Here the variation of the laser intensity over the dimensions of the lattice created spatially dependent hopping terms. The drawback of this method is the restriction to only a Gaussian variation of the tunneling operators and no control over this feature can be exerted. This significantly limits the freedom of realizing various metrics for the curved space Hamiltonian.

We investigate the nature of the LDOS for the Hamiltonian in equation (26) and look for the imprint of spatial curvature in its behavior. The LDOS computations are performed for the choice of the driving scheme given in equation (31). The expressions in equations (28) and (30) are evaluated numerically to estimate the LDOS. Figure 1 shows the modification to the LDOS for our system over that of normal graphene in flat space. The figure shows the quantity $(\rho/\rho_0) - 1$ plotted in the color contour map against the spatial coordinates x and y. As seen in the figure, a large positive correction is centered at the reference origin indicating maximum increase in the number of available states per unit energy. This is a clear indication that electronic properties are significantly altered in our system. An 80% correction is observed at the maxima for our choice of driving frequency which yields a ω^{-1} of ∼0.01. We note that a similar behavior of the LDOS has also been observed in the study of graphene in curved space with positive curvature [51–54].

4 Conclusion

We conclude by noting that the use of periodic forcing to generate the effects of curved space on 2D quantum systems has a far reaching influence in theoretical studies and technological applications. The traditional Floquet analysis of periodically driven systems uses the CBH/Trotter expansion to find the effective static Hamiltonians. We use an alternative perturbative formulation using a pulsed driving scheme and find an effective approximate Hamiltonian. We show that the driving scheme can be chosen to simulate tunable geometric properties of curved space. Our work particularly studies an optical lattice analogue for graphene in curved space. The massless Dirac equation and Hamiltonian in curved space, that model electronic behavior in curved graphene, are derived for a conformal metric. The same is shown to be obtained in a periodically driven fermionic optical lattice having chosen the appropriate modulating operators. We go on to analyze the geometrical and physical features of the system, namely, the Gauss curvature and LDOS. These are computed for a particular choice of metric and deviations from the unperturbed system are noted. This opens up the possibility of synthesis of new systems in quantum simulators and the study of their physical properties.

Appendix

The approach outlined here is based on earlier works [26,28]. Time evolution of a state $\psi(t)$ is given by:

$$i\frac{\partial\psi}{\partial t} = \hat{H}\psi \tag{A.1}$$

where $\hat{H} = \hat{H}(t)$. The evolution of an initial state $\psi(t_i) = \psi_i$ to a final state $\psi(t_f) = \psi_f$ is governed by a Unitary operator $U(t_i, t_f)$ such that $\psi_f = U(t_i, t_f)\psi_i$. The Hamiltonian under consideration is of the form

$$\hat{H}(t) = \hat{H}_o + \hat{V}(t). \tag{A.2}$$

Integrating equation (A.1) is not trivial since the Hamiltonian at different times do not commute. Standard perturbation methods are also only applicable when the potential is a weak correction. We are interested in potentials that are periodic in time

$$\hat{V}(t): \qquad \hat{V}(t+T) = \hat{V}(t). \tag{A.3}$$

Let us define a Unitary transformation $\hat{\mathcal{U}}(t)$

$$\hat{\mathcal{U}}: \quad \psi(t) \to \hat{\mathcal{U}}\psi(t) = \phi(t).$$

Such that $\phi(t)$ satisfies

$$i\frac{\partial\phi(t)}{\partial t} = \hat{H}_{eff}\phi(t), \tag{A.4}$$

where $\hat{H}_{eff}$ is to be made to be time-independent. We seek an operator $\hat{\mathcal{U}}(t) = e^{i\hat{F}(t)}$ (where $\hat{F}(t)$ is Hermitian)

such that $\phi(t) = \hat{\mathcal{U}}(t)\psi(t)$, evolves under an effective time independent Hamiltonian $\hat{H}_{eff}$. Therefore we have,

$$i\frac{\partial}{\partial t}\left(\hat{\mathcal{U}}\psi(t)\right) = \hat{H}_{eff}\hat{\mathcal{U}}\psi(t), \tag{A.5}$$

and

$$\hat{\mathcal{U}}(t) = e^{i\hat{F}(t)}, \tag{A.6}$$

which upon further evaluation yields

$$\hat{H}_{eff} = e^{i\hat{F}(t)}\hat{H}e^{-i\hat{F}(t)} + i\frac{\partial}{\partial t}\left(e^{i\hat{F}(t)}\right)e^{-i\hat{F}(t)}. \tag{A.7}$$

All the time dependence is pushed to the operator $\hat{F}(t)$ and $\hat{H}_{eff}$ is rendered time-independent. For an evolution from $t_i \to t_f$, we therefore have a trivial evolution

$$\phi(t_f) = e^{-i\hat{H}_{eff}(t_f - ti)}\phi(t_i). \tag{A.8}$$

Since, $\phi(t_f) = e^{i\hat{F}(t_f)}\psi(t_f)$ and $\phi(t_i) = e^{i\hat{F}(t_i)}\psi(t_i)$, we have $U : \psi_i \to \psi_f$ given by:

$$U(t_i, t_f) = e^{-i\hat{F}(t_f)}e^{-i\hat{H}_{eff}(t_f - t_i)}e^{i\hat{F}(t_i)}. \tag{A.9}$$

Here, $\hat{F}(t)$ is a time dependent Hermitian operator with $\hat{F}(t+T) = \hat{F}(t)$. It is important to note here that $\hat{H}_{eff}$ is independent of both t_i and t_f, which have been transferred into the "Kick" terms $e^{i\hat{F}(t_i)}$ and $e^{-i\hat{F}(t_f)}$ respectively. It is generally not possible to extract the operators $\hat{F}(t)$ and $\hat{H}_{eff}$ in closed analytic form except for some special cases. However, if the driving frequency $\omega = 2\pi/T$ is high, one can consider a perturbative expansion using the small parameter $1/\omega$. The expansions for $\hat{H}_{eff}$ and $\hat{F}$ are

$$\hat{H}_{eff} = \sum_{0\le n<\infty}\frac{1}{\omega^n}\hat{H}^{(n)} \quad \hat{F} = \sum_{1\le n<\infty}\frac{1}{\omega^n}\hat{F}^{(n)}. \tag{A.10}$$

The prescription to obtain the effective Hamiltonian is as follows.

a. Write equation (A.7) for $\hat{H}_{eff}$ as an expanded perturbation series in $(\frac{1}{\omega})$.
b. At each order of perturbation, which corresponds to a specific power of $(\frac{1}{\omega})$, retain the time-independent average (taken over one time-period T) in $\hat{H}_{eff}$ and adjust $\hat{F}$ to annihilate any time dependence.
c. Repeat the procedure at each order in perturbation.

The following identities are of help in following the above prescription

$$e^{i\hat{F}}\hat{H}e^{-i\hat{F}} = \hat{H} + i\left[\hat{F},\hat{H}\right] - \frac{1}{2}\left[\hat{F},\left[\hat{F}'\hat{H}\right]\right] - \frac{i}{6}\left[\hat{F},\left[\hat{F},\left[\hat{F},\hat{H}\right]\right]\right] + \ldots \tag{A.11}$$

and

$$\left(\frac{\partial}{\partial t}e^{\hat{F}}\right)e^{-i\hat{F}} = i\frac{\partial\hat{F}}{\partial t} - \frac{1}{2}\left[\hat{F},\frac{\partial\hat{F}}{\partial t}\right] - \frac{i}{6}\left[\hat{F},\left[\hat{F},\frac{\partial\hat{F}}{\partial t}\right]\right] + \ldots \tag{A.12}$$

Expanding the potential in Fourier series, we have

$$\widehat{V}(t) = \widehat{V}_0 + \sum_{n=1}^{\infty}\left(\widehat{V}_n e^{in\omega t} + \widehat{V}_{-n}e^{-in\omega t}\right). \tag{A.13}$$

Substituting $\hat{H}_{eff} = \sum_{0\le n<\infty}\frac{1}{\omega^n}\hat{H}^{(n)}$ and $\hat{F} = \sum_{1\le n<\infty}\frac{1}{\omega^n}\hat{F}^{(n)}$ in equation (A.7), and using equations (A.11) and (A.12), the prescription given above gives us up to $\mathcal{O}(1/\omega^2)$:

$$\begin{aligned}
\widehat{H}_{eff} &= \widehat{H}_0 + \widehat{V}_0 + \frac{1}{\omega}\sum_{n=1}^{\infty}\frac{1}{n}\left[\widehat{V}_n,\widehat{V}_{-n}\right] \\
&+ \frac{1}{2\omega^2}\sum_{n=1}^{\infty}\frac{1}{n^2}\left(\left[\left[\widehat{V}_n,\widehat{H}_0\right],\widehat{V}_{-n}\right] + \text{h.c.}\right) \\
&+ \frac{1}{3\omega^2}\sum_{n,m=1}^{\infty}\frac{1}{nm}\left(\left[\widehat{V}_n,\left[\widehat{V}_m,\widehat{V}_{-n-m}\right]\right]\right. \\
&\left. - 2\left[\widehat{V}_n,\left[\widehat{V}_{-m},\widehat{V}_{m-n}\right]\right] + \text{h.c.}\right) \\
\widehat{F}(t) &= \frac{1}{i\omega}\sum_{n=1}^{\infty}\frac{1}{n}\left(\widehat{V}_n e^{in\omega t} - \widehat{V}_{-n}e^{-in\omega t}\right) \\
&+ \frac{1}{i\omega^2}\sum_{n=1}^{\infty}\frac{1}{n^2}\left(\left[\widehat{V}_n,\widehat{H}_0 + \widehat{V}_0\right]e^{in\omega t} - \text{h.c.}\right) \\
&+ \frac{1}{2i\omega^2}\sum_{n,m=1}^{\infty}\frac{1}{n(n+m)}\left([\widehat{V}_n,\widehat{V}_m]e^{i(n+m)\omega t} - \text{h.c.}\right) \\
&+ \frac{1}{2i\omega^2}\sum_{n\ne m=1}^{\infty}\frac{1}{n(n-m)}\left(\left[\widehat{V}_n,\widehat{V}_{-m}\right]e^{i(n-m)\omega t} - \text{h.c.}\right).
\end{aligned} \tag{A.14}$$

This general expression for the approximate effective static Hamiltonian for periodically driven systems is used in the article.

References

1. I. Bloch, J. Dalibard, W. Zwerger, Rev. Mod. Phys. **80**, 885 (2008)
2. Y.J. Lin, R.L. Compton, A.R. Perry, W.D. Phillips, J.V. Porto, I.B. Spielman, Phys. Rev. Lett. **102**, 130401 (2009)
3. M. Greiner, O. Mandel, T. Esslinger, T. Hänsch, I. Bloch, Nature **415**, 39 (2002)
4. Z. Hadzibabic, P. Krüger, M. Cheneau, B. Battelier, J. Dalibard, Nature **441**, 1118 (2006)
5. M. Grifoni, P. Hänggi, Phys. Rep. **304**, 229 (1998)

6. J. Dalibard, F. Gerbier, G. Juzeliūnas, P. Öhberg, Rev. Mod. Phys. **83**, 1523 (2011)
7. M.A.H. Vozmediano, M.I. Katsnelson, F. Guinea, Phys. Rep. **496**, 109 (2010)
8. F. de Juan, J.L. Mañes, M.A.H. Vozmediano, Phys. Rev. B **87**, 165131 (2013)
9. J.L. Mañes, F. de Juan, M. Sturla, M.A.H. Vozmediano, Phys. Rev. B **88**, 155405 (2013)
10. F. Guinea, M.I. Katsnelson, A.K. Geim, Nat. Phys. **6**, 30 (2010)
11. P. San-Jose, J. Gonzalez, F. Guinea, Phys. Rev. Lett. **108**, 216802 (2012)
12. A.S. Sorensen, E. Demler, M.D. Lukin, Phys. Rev. Lett. **94**, 086803 (2005)
13. L.K. Lim, C.M. Smith, A. Hemmerich, Phys. Rev. Lett. **100**, 130402 (2008)
14. A. Hemmerich, Phys. Rev. A **81**, 063626 (2010)
15. C.E. Creffield, F. Sols, Phys. Rev. A **84**, 023630 (2011)
16. A. Bermudez, T. Schaetz, D. Porras, Phys. Rev. Lett. **107**, 150501 (2011)
17. J. Struck, C. Ölschläger, M. Weinberg, P. Hauke, J. Simonet, A. Eckardt, M. Lewenstein, K. Sengstock, P. Windpassinger, Phys. Rev. Lett. **108**, 225304 (2012)
18. P. Hauke, O. Tieleman, A. Celi, C. Ölschläger, J. Simonet, J. Struck, M. Weinberg, P. Windpassinger, K. Sengstock, M. Lewenstein, A. Eckardt, Phys. Rev. Lett. **109**, 145301 (2012)
19. B.M. Anderson, I.B. Spielman, G. Juzeliūnas, Phys. Rev. Lett. **111**, 125301 (2013)
20. A. Nauts, R.E. Wyatt, Phys. Rev. A **30**, 872 (1984)
21. M.M. Maricq, Phys. Rev. B **25**, 6622 (1982)
22. J.H. Shirley, Phys. Rev. **138**, 979 (1965)
23. H. Sambe, Phys. Rev. A **7**, 2203 (1973)
24. T.P. Grozdanov, M.J. Rakovic, Phys. Rev. A **38**, 1739, (1988)
25. P. Avan, C. Cohen-Tannoudji, J. Dupont-Roc, C. Fabre, J. Phys. **37**, 993 (1976)
26. S. Rahav, I. Gilary, S. Fishman, Phys. Rev. A **68**, 013820 (2003)
27. J.N. Bandyopadhyay, T. Guha Sarkar, Phys. Rev. E **91**, 032923 (2015)
28. N. Goldman, J. Dalibard, Phys. Rev. X **4**, 031027 (2014)
29. A.H. Castro Neto, F. Guinea, N.M.R. Peres, K.S. Novoselov, A.K. Geim, Rev. Mod. Phys. **81**, 109 (2009)
30. I. Bloch, Nat. Phys. **1**, 23 (2005)
31. M. Wilson, Phys. Today **59**, 21 (2006)
32. A.C. Neto, F. Guinea, N.M. Peres, Phys. World **19**, 33 (2006)
33. S.Y. Zhou, G.-H. Gweon, J. Graf, A.V. Fedorov, C.D. Spataru, R.D. Diehl, Y. Kopelevich, D.-H. Lee, S.G. Louie, A. Lanzara, Nat. Phys. **2**, 595 (2006)
34. S.L. Zhu, B. Wang, L.-M. Duan, Phys. Rev. Lett. **98**, 260402 (2007)
35. K.L. Lee, B. Grémaud, R. Han, B.-G. Englert, C. Miniatura, Phys. Rev. A **80**, 043411 (2009)
36. J.M. Hou, W.-X. Yang, X.-J. Lou, Phys. Rev. A **79**, 043621 (2009)
37. G. Juzeliūnas, J. Ruseckas, M. Lindberg, L. Santos, P. Öhberg, Phys. Rev. A **77**, 011802(R) (2008)
38. B. Wunsch, F. Guinea, F. Sols, New J. Phys. **10**, 103027 (2008)
39. R. Shen, L.B. Shao, B. Wang, D.Y. Xing, Phys. Rev. B **81**, 041410 (2010)
40. K. Asano, C. Hotta, Phys. Rev. B **83**, 245125 (2011)
41. L. Tarruell, D. Greif, T. Uehlinger, G. Jotzu, T. Esslinger, Nature **483**, 302 (2012)
42. M. Polini, F. Guinea, M. Lewenstein, H.C. Manoharan, V. Pellegrini, Nat. Nanotechnol. **8**, 625 (2013)
43. G. Jotzu, M. Messer, R. Desbuquois, M. Lebrat, T. Uehlinger, D. Greif, T. Esslinger, Nature **515**, 237 (2014)
44. S.E. Savel'ev, W. Häusler, P. Hänggi, Eur. Phys. J. B **86**, 433 (2013)
45. S. Savel'ev, W. Häusler, P. Hänggi, Phys. Rev. Lett. **109**, 226602 (2012)
46. J. Gonzalez, F. Guinea, M.A.H. Vozmediano, Phys. Rev. Lett. **69**, 172 (1992)
47. F. de Juan, A. Cortijo, M.A.H. Vozmediano, Phys. Rev. B **76**, 165409 (2007)
48. A. Cortijo, F. Guinea, M.A.H. Vozmediano, J. Phys. A **45**, 383001 (2012)
49. A. Iorio, Ann. Phys. **326**, 1334 (2011)
50. A. Iorio, G. Lambiase, Phys. Lett. B **716**, 334 (2012)
51. A. Cortijo, M.A.H. Vozmediano, Eur. Phys. J. Special Topics **148**, 83 (2007)
52. A. Cortijo, M.A.H. Vozmediano, Europhys. Lett. **77**, 47002 (2007)
53. A. Cortijo, M.A.H. Vozmediano, Nucl. Phys. B **763**, 293 (2007)
54. A. Cortijo, M.A.H. Vozmediano, Phys. Rev. B **79**, 184205 (2009)
55. F. Guinea, M.I. Katsnelson, M.A.H. Vozmediano, Phys. Rev. B **77**, 075422 (2008)
56. O. Boada, A. Celi, J.I. Latorre, M. Lewenstein, New J. Phys. **13**, 035002 (2011)
57. I.I. Satija, D.C. Dakin, J.Y. Vaishnav, C.W. Clark, Phys. Rev. A **77**, 043410 (2008)
58. D. Jaksch, P. Zoller, New J. Phys. **5**, 56 (2003)
59. G. Juzeliūnas, J. Ruseckas, P. Öhberg, M. Fleischhauer, Phys. Rev. A **73**, 025602 (2006)
60. K.J. Günter, M. Cheneau, T. Yefsah, S.P. Rath, J. Dalibard, Phys. Rev. A **79**, 011604(R) (2009)
61. N. Goldman, A. Kubasiak, P. Gaspard, M. Lewenstein, Phys. Rev. A **79**, 023624 (2009)
62. J. Ruseckas, G. Juzeliūnas, P. Öhberg, M. Fleischhauer, Phys. Rev. Lett. **95**, 010404 (2005)
63. N. Goldman, A. Kubasiak, A. Bermudez, P. Gaspard, M. Lewenstein, M.A. Martin-Delgado, Phys. Rev. Lett. **103**, 035301 (2009)
64. J. Dalibard, F. Gerbier, G. Juzeliūnas, P. Öhberg, Rev. Mod. Phys. **83**, 1523, (2011)
65. P. Soltan-Panahi, J. Struck, P. Hauke, A. Bick, W. Plenkers, G. Meineke, C. Becker, P. Windpassinger, M. Lewenstein, K. Sengstock, Nat. Phys. **7**, 434 (2011)
66. J. Struck, C. Ölschläger, R. Le Targat, P. Soltan-Panahi, A. Eckardt, M. Lewenstein, P. Windpassinger, K. Sengstock, Science **333**, 996 (2011)
67. P. Hauke, O. Tieleman, A. Celi, C. Ölschläger, J. Simonet, J. Struck, M. Weinberg, P. Windpassinger, K. Sengstock, M. Lewenstein, A. Eckardt, Phys. Rev. Lett. **109**, 145301 (2012)
68. J. Struck, M. Weinberg, C. Ölschläger, P. Windpassinger, J. Simonet, K. Sengstock, R. Höppner, P. Hauke, A. Eckardt, M. Lewenstein, L. Mathey, Nat. Phys. **9**, 738 (2013)
69. M.D. Pollock, Acta Physica Polonica B **41**, 1827 (2010)
70. Y. Sucu, N. Unal, J. Math. Phys. **48**, 052503 (2007)

71. V.R. Khalilov, C.-L. Ho, Mod. Phys. Lett. A **13**, 615 (1998)
72. V.R. Khalilov, C.-L. Ho, Chinese J. Phys. **47**, 294 (2009)
73. C.-L. Ho, V.R. Khalilov, Phys. Rev. A **61**, 032104 (2000)
74. S.P. Gavrilov, D.M. Gitman, A.A. Smirnov, Eur. Phys. J. C **32**, 119 (2003)
75. S.P. Gavrilov, D.M. Gitman, Phys. Rev. D **53**, 7162 (1996)
76. P.D. Gupta, S. Raj, D. Chaudhuri, `arXiv:1012.0976` (2010)
77. L. Menculini, O. Panella, P. Roy, Phys. Rev. D **87**, 065017 (2013)
78. D.R. Brill, J.A. Wheeler, Rev. Mod. Phys. **29**, 465 (1957)
79. L.D. Landau, E.M. Lifshitz, *Mechanics*, 3rd edn. (Pergamon, Oxford, 1976), Sect. 30
80. I.C. Percival, D. Richards, *Introduction to Dynamics* (Cambridge University Press, London, 1982), p. 153
81. A. Bacsi, A. Virosztek, Phys. Rev. B **82**, 193405 (2010)
82. G. Gui, J. Lin, J. Zhong, Phys. Rev. B **78**, 075435 (2008)
83. M.Y. Han, B. Özylimaz, Y. Zhang, P. Kim, Phys. Rev. Lett. **98**, 206805 (2007)
84. I. Snyman, Phys. Rev. B **80**, 054303 (2009)
85. R.P. Tiwari, D. Stroud, Phys. Rev. B **79**, 205435 (2009)
86. C. Coletti, C. Riedl, D.S. Lee, B. Krauss, L. Patthey, K. von Klitzing, J.H. Smet, U. Starke, Phys. Rev. B **81**, 235401 (2010)
87. K.K. Gomes, W. Mar, W. Ko, F. Guinea, H.C. Manoharan, Nature **483**, 306 (2012)
88. F.D.M. Haldane, Phys. Rev. Lett. **61**, 2015 (1988)
89. I.F. Herbut, Phys. Rev. B **78**, 205433 (2008)
90. S. Zhu, Y. Huang, N.N. Klimov, D.B. Newell, N.B. Zhitenev, J.A. Stroscio, S.D. Solares, T. Li, Phys. Rev. B **90**, 075426 (2014)
91. J.L. Mañes, F. Guinea, M.A.H. Vozmediano, Phys. Rev. B **75**, 155424 (2007)
92. R. de Gail, J.-N. Fuchs, M.O. Goerbig, F. Piéchon, G. Montambaux, Physica B **407**, 1948 (2012)
93. Y. Aharonov, J. Anandan, Phys. Rev. Lett. **58**, 1593 (1987)
94. J. Struck, J. Simonet, K. Sengstock, Phys. Rev. Lett. **90**, 031601(R) (2014)